



Long-Term Continuous Anaerobic Co-digestion of Residual Biomass—Model Validation and Model-Based Investigation of Different Carbon-to-Nitrogen Ratios

Jana Schultz¹ · Marvin Scherzinger¹ · Amr Y. Elbanhawy² · Martin Kaltschmitt¹

Received: 5 November 2024 / Accepted: 26 May 2025
© The Author(s) 2025

Abstract

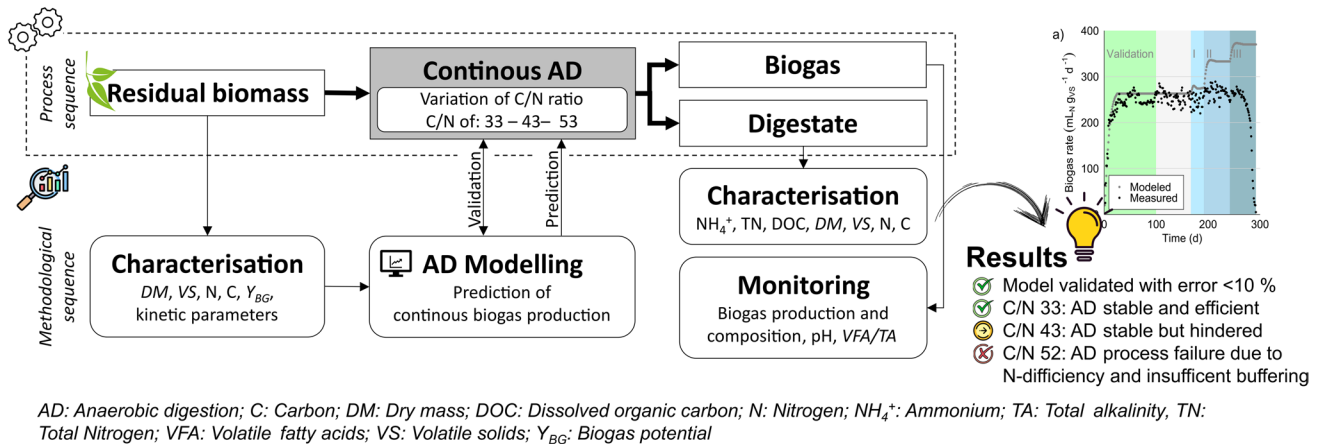
Major challenges in using lignocellulosic residues as biogas substrates arise from their high diversity and their typically low nitrogen content, which may not provide sufficient nitrogen for the microorganisms. To investigate to what extent such substrates can be used in biogas plants without extensive pre-treatment, this study presents a 300-day continuous co-digestion of lignocellulosic substrates (i.e., sugarcane reed, lemon, and grape leaves) and goat manure while continuously monitoring various process parameters. The results suggest a stable and effective biogas production at a carbon-to-nitrogen ratio (C/N ratio) of 33, with a production of $244 \pm 15 \text{ mL}_N \text{ g}_{VS}^{-1} \text{ d}^{-1}$ biogas. At a higher C/N ratio of 43, the process remained stable, but hindrance was encountered. Process failure occurred at a C/N ratio of 52, where a rapid decline in biogas production was observed, accompanied by an increase in the volatile fatty acids to total alkalinity ratio (from < 0.2 to 0.9), a drop in the pH-value (from > 7 to 5.4), and an increased CO_2 -content of the provided biogas (from $> 50\%$ to 43%). The compositional analysis of the digestate suggests an insufficient N-supply and a failure of the carbonate and ammonium buffer systems inside the reactor. The experiment also served to validate a previously developed model based on the individual substrates' degradation kinetics. With a relative root mean square error *rRMSE* of 8%, the model adequately predicted biogas production within defined limits. However, it could not anticipate process breakdown at high C/N ratios, highlighting a strong limitation.

Highlights

- First-time validation of an accessible kinetics-based model for anaerobic digestion
- Long-term stable continuous anaerobic digestion of Egyptian lignocellulosic residues
- Assessment of restrictions in terms of C/N ratio as indication of nitrogen supply
- Demonstration of feasibility and limits of the use of lignocellulosic substrates

Extended author information available on the last page of the article

Graphical Abstract



Keywords Biogas · Biomethane · Agricultural residues · Lignocellulosic biomass · Digestate · Modeling

Introduction

The sustainability of biogas production processes depends largely on the biogenic resources used as substrates. The cultivation of energy crops is often related to intensive land use and a corresponding loss of biodiversity [1]. Contrastingly, the use of organic residues from agriculture (e.g., straw, manure) and municipalities (e.g., biowaste) not only mitigates such problems but also functions as a form of waste management. Agricultural residues and animal manure represent the largest sources of renewable feedstocks for biogas production [2]. Remarkably, the sustainable technical potential of biogas and biomethane from these sources are estimated to range around 6600 TWh a^{-1} and 8500 TWh a^{-1} , respectively [2] being considerably higher compared to the current production of 445 TWh in 2022 [3] as well as the projected demand of 1700 TWh (Stated Policies Scenario) to 3800 TWh (Sustainable Development Scenario) in 2040 [2].

Lignocellulosic biomass constitutes the largest fraction of agricultural residues and is widely available as a potential feedstock for anaerobic digestion. The versatility of biogas in terms of location/region, substrates used, and size of the fermenter (from lab-scale to large plants) is an enormous advantage in terms of flexibility. This includes the use of small-scale biogas plants in rural areas for decentralized, local production of renewable energy. However, the variety of possible applications is also a challenge. For instance, because lignocellulosic residues have diverse characteristics, operating a biogas plant with such substrates is not necessarily straightforward. Despite public promotion, small-scale biogas plants in rural areas are often operated inefficiently or

not adopted by farmers [4]. A key challenge is the fluctuating composition and properties of locally, regionally, and seasonally available lignocellulosic biomass streams. Also, those substrates exhibit recalcitrance toward anaerobic degradation, resulting from their biomass structure and considerable content of non-degradable lignin [5, 6]. The nutrient supply provided by the substrate, e.g., the carbon-to-nitrogen (C/N) ratio, not only varies from substrate to substrate but can also be subject to seasonal changes, for example, as seen in food waste [7]. Lignocellulosic biomass itself is usually characterized by a low N content, resulting in an inadequate C/N ratio for anaerobic digestion.

An adequate C/N ratio needs to be maintained because microorganisms realizing the anaerobic digestion use carbon as their main source of energy and nitrogen to build up amino acids and proteins [8]. Nitrogen is taken up by these microorganisms in the form of NH_4^+ from the digestate [9]. In this context, there are two possible challenges.

- If the C/N ratio is low, ammonium inhibition might emerge due to excessive NH_4^+ availability [8, 10]. This can be the case when food waste or municipal solid organic waste [8, 11] or large quantities of animal manure [10] are used as feedstock.
- If the C/N ratio is high (i.e., only little nitrogen is available), the protein solubilization rates are low, and consequently, NH_4^+ concentrations are also rather low, thus providing insufficient N to maintain cell growth of microorganisms [10]. This could then result in a reduced amount of microorganisms available within the system and hinder the build-up or preservation of the microbial

flora, which could in turn slow down the biogas production process [12], and ultimately means that the available C would be used inefficiently [10]. Additionally, since the ammonium buffer (equilibrium of ammonium and ammonia) is one of the major buffering systems besides the carbonate buffer [13], an insufficiently low NH_4^+ concentration weakens the buffering capacity of the biogas reactor. This makes the system more susceptible to overacidification [8, 14] and thus could lead to significant changes in the pH-value, which could ultimately slow down or stop cell growth [15].

Under mesophilic conditions, optimal C/N ratios for anaerobic digestion have been found to lie between 20 and 35 [10, 16, 17]. Inhibition due to excess NH_4^+ is likely to occur at C/N ratios below 15 [16]. Higher C/N ratios might lead to hindrance or failure of the biogas production as a consequence of N-deficiency—even though stable anaerobic production processes have been reported at C/N ratios up to 60 [18, 19].

Since the more prominent problem in biogas plant operation are low C/N ratios (high NH_4^+ concentrations), various papers document the positive effect of a *higher* C/N ratio (in comparison to pure animal manure but often lower than lignocellulosic residues) on biogas production [20, 21], which however is also challenged by contradicting observations [19, 22]. It is not always analyzed whether the additional biogas results from the improved C/N ratio or simply from the use of a substrate mixture containing higher proportions of substrates with a higher biogas potential. Furthermore, batch tests are often employed to study these effects [23] rather than performing long-term experiments with continuous substrate feeding. Moreover, many studies use substrates that inherently contain microorganisms able to perform anaerobic digestion (e.g., fresh dairy manure) [18, 20]. The continuous addition of these microorganisms may compensate for a potential collapse of the microbial community. Even though considerably scarcer than batch tests, some long-term studies of continuous biogas processes can be found in the literature. For example, various pre-treatment methods (extrusion, lime pre-treatment, steam explosion) have already been tested on a continuous scale. In these studies, various lignocellulosic materials, such as rice straw, corn stover and straw, or lignin-rich macrophytes, have been used, often with the addition of N-rich substrates such as pig manure or food waste [24–27]. Moreover, to improve anaerobic conversion, pre-hydrolysis [28] and enzyme addition were investigated on a continuous scale [29]. Blends of lignocellulosic agricultural residues with different C/N ratios were used for anaerobic digestion in a study by Zahan et al. [21]. However, the variation of the C/N ratio did not exceed 25, thus maintaining favorable conditions without overexpansion. Overall, continuous long-term processes with high

C/N ratios—as high as those of lignocellulosic residues from agriculture—are scarce and their dynamics are generally less well understood than the opposite case of low C/N ratios with excess nitrogen.

Modern anaerobic digestion research and development is greatly supported by mathematical modeling of anaerobic processes. On the one hand, they enable a detailed understanding of processes and, on the other hand, they can support technical implementation and plant operation. The research landscape includes a variety of models [30–32], which can be categorized based on their modeling approach into mechanistic, kinetic, and phenomenological models [31]. Mechanistic models seek to depict physical, biological, and chemical processes in the anaerobic reactor, relying on a large number of input parameters that need to be determined experimentally [31]. Even though, for example, the “Anaerobic digestion model No. 1” (ADM1) is well known and widely applied in research, it comprises great complexity [30, 33] which is not always well suited for simple applications, especially when the target applicant is not the scientific community but practitioners operating plants. Machine learning models, e.g., models based on artificial neural networks (ANN) [30, 34] are referred to as phenomenological models [31]. Unlike for mechanistic models, precise knowledge of the bio-physio-chemical mechanisms inside the reactor is not needed. However, phenomenological models heavily rely on large input data sets for training and prediction [31]. Kinetic models determine the biogas production of a system via empirical equations, specifically enzymatic or canonical algebraic equations, that use dimensionless coefficients [35]. This approach can be considerably easier to implement and use because phenomenological models have high data requirements, and mechanistic models are inherently complex.

Following this line of argument and to facilitate a successful and stable operation of (e.g., small-scale) plants using a variety of different renewable feedstocks, Scherzinger et al. [33] developed an empirical model that uses simple means to check the viability of the proposed substrate mix and predict the respective biogas yield in a continuous biogas production process. Their model is characterized by an easy approach using the degradation kinetics of the substrates. It checks for an appropriate C/N ratio and takes some framework conditions (e.g., the maximum organic loading rate) into account [33]. Because it uses basic characteristics, it is easily transferable and adaptable to a large share of substrates. The proposed model has not yet been validated by continuous anaerobic digestion experiments. In their publication, the authors assumed that the prediction would be accurate under favorable conditions, such as an adequate C/N ratio, while the model is not designed to predict process hindrances and breakdowns. Consequently, they recommended that the use of the model should be limited to applications within the

borders of favorable conditions [33]. The model’s unknown predictive limits justify further investigations.

Against this background, this paper has the following main objectives:

- The biogas production from selected N-deficient lignocellulosic residues was examined in a co-digestion with animal manure. Given the limited availability of N-rich manure in parts of the study area (i.e., Egypt), the target was to minimize its use while utilizing lignocellulosic residues as efficiently as possible. Throughout the experiment, manure input was gradually reduced to assess the impact of a varied C/N ratio of the substrate mix on biogas production and selected digestate characteristics. To provide robust and reliable results, this study included long-term observations spanning several months, capturing the effects of substrate changes over time.
- The above-described predictive model was validated using data from a continuously fed biogas reactor. The model predictions were checked against the experimental biogas production. Since the model was expected only to perform well under optimal conditions, deviations from ideal conditions were introduced. This should demonstrate that the model (or more precisely the deviation

from the model’s prediction) can indicate process inhibition at an early stage, which could enable rapid intervention in practice.

In summary, this study presents the first-time validation of the predictive model by Scherzinger et al. [33] in continuous mode. Building upon this model, the present investigation expands the state of the art in the field of empirical models for the prediction of anaerobic processes, as well as the use of N-deficient key agricultural residues in biogas production processes.

Materials and Methods

Procedure

To adequately address the two goals of the study, namely, the model validation and the assessment of a varied C/N ratio in the substrate mix (C/N_{feed}), the study was composed of different phases as outlined in Fig. 1 and Table 1. The process sequence (Fig. 1) is a representation of the biogas process itself, showing the conversion from residual biomass to biogas and digestate through anaerobic digestion with continuous substrate feeding.

Fig. 1 Experimental procedure. AD: anaerobic digestion; C: carbon; DM: dry mass; DOC: dissolved organic carbon; H: hydrogen; N: nitrogen; NH_4^+ : ammonium; O: oxygen; S: sulfur; TA: total alkalinity; TN: total Nitrogen; VFA: volatile fatty acids; VS: volatile solids; Y_{BG} : biogas potential

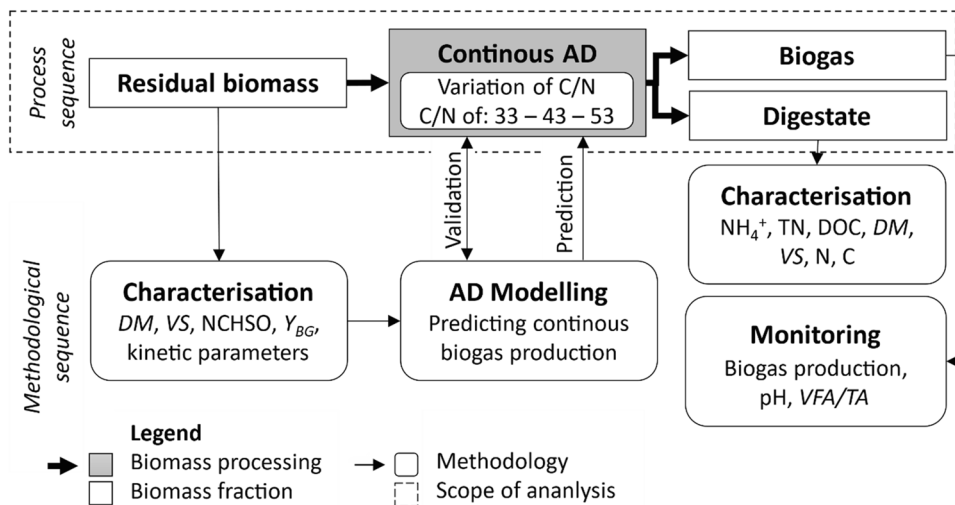


Table 1 Feedstock blends: shares of substrates in %_{VS} (% of volatile solids) of each study phase. C/N_{feed} is the C/N ratio of the final substrate mix. Duration gives the start and end day, as well as the total duration in brackets

Phase	Agricultural residues		Manure	C/N_{feed}	Duration day (d)
	% _{VS}	% _{VS}			
Validation	Sugarcane reed I	Lemon leaves	Goat dung	33	0–99 (75 + 25)
	25	25	50		
Transition	25	25	50	33	100–166 (67)
I	Sugarcane reed II	Grape leaves	Goat dung	33	167–191 (25)
	25	25	50		
	40	40	20		
III	50	50	0	52	242–291 (50)

The methodological sequence is composed of the characterization of the residual biomass (“**Characterization of Substrates**” section), the modeling of the anaerobic digestion processes (“**Modeling of the Continuous Digestion Process**” section) including the model validation and the prediction of the biogas production, and lastly, a characterization of the digestate and constant monitoring of process parameters during the entire operation of the biogas process (“**Continuous Anaerobic Co-digestion**” section).

The study was divided into multiple phases. Table 1 shows an overview of the feedstock and the respective C/N_{feed} ratio of the substrate mix used during the different study phases as well as the respective duration of the different phases.

The validation phase was run to validate the model for the prediction of the anaerobic digestion process. The startup of this phase lasted for 75 days to ensure a steady state of the anaerobic digestion process (this equals three hydraulic retention times (HRT) of 25 d, see also Eq. (8)) and continued until day 99. During this phase, the reactor used for anaerobic digestion was fed with a blend of 50% $_{VS}$ agricultural residues (sugarcane reed I and lemon leaves in equal amounts) and 50% $_{VS}$ goat dung. Between the validation phase and the other three major phases, there was a transition period. During this time, the plant was continuously operated; however, due to operational difficulties (i.e., reactor handling, gas collection, data acquisition), which led to an incomplete data set in this phase, the results of the transition phase are not used for discussion.

In the follow-up phases I, II, and III, the effect of a varied C/N_{feed} ratio was tested by altering it. During these phases, the agricultural residues used were sugarcane reed II (originating from a different batch and thus showing different characteristics than the sugarcane reed I), grape leaves, and goat dung. The variation of the substrates has the additional advantage that the model validity and process stability have been tested using different substrates. Over a period of one HRT (phase I; $HRT = 25$ d, see also Eq. (8)) or two HRT (phases II and III) each, the reactor was operated with a blend of agricultural residues and manure at different proportions. Phase I was run under the same conditions as the validation phase using 50% $_{VS}$ agricultural residues and 50% $_{VS}$ manure. The share of manure was then reduced to 20% $_{VS}$ in phase II and to 0% $_{VS}$ in phase III. These different feedstock blends corresponded to a C/N_{feed} ratio of 33 (phase I), 43 (phase II), and 52 (phase III).

Substrates for Anaerobic Digestion

Selection and Preparation of Substrates

The selection of substrates for continuous anaerobic digestion from a pool of crop residues from different governorates

in Egypt was based on seasonal and regional availability and their biogas potential. The substrates chosen originate from the region of Aswan in the south of Egypt. Here, they are available in the winter season. According to a qualitative field survey [36], the residues chosen are often subject to field burning [37]. Hence, there is low competition for use, making these materials potentially favorable biogas substrates.

As the agricultural residues investigated mostly consisted of biomass with high C/N ratios, the substrate mix was supplemented by goat dung as a N-rich substrate. It was dried in a ventilated oven at 45 °C for 2 d to prevent microbial activity or degradation during storage. A sandy fraction was separated and removed from the goat dung by sieving.

The substrates were comminuted to a particle size < 1 mm using a laboratory cutting mill (MF10, IKA, Germany) for the subsequent characterization and the batch and continuous anaerobic digestion experiments.

Characterization of Substrates

Dry Mass and Volatile Solid Content Dry mass and volatile solids content were determined according to DIN EN ISO 18134 [38] and DIN EN 15935 [39]. The drying for the determination of the water content was carried out in a drying oven (U80, Memmert, Germany) at 105 °C. Subsequently, the ashing of the samples for volatile solid determination took place in a muffle furnace (M104, Thermo Scientific Heraeus, USA) at 550 °C. The dry mass content (DM) and the volatile solids content (VS) were calculated based on Eqs. (1) and (2).

$$DM = (m_d/m_f)100\% \quad (1)$$

$$VS = (1 - (m_a/m_d))100\% \quad (2)$$

m_f is the fresh mass of the sample before drying, m_d is the mass of the dry sample, and m_a is the mass of the ash after incineration. Measurements were carried out in triplicates.

Elemental Composition The elements nitrogen (N), carbon (C), hydrogen (H), and sulfur (S) were determined with a NCHS analyzer with an internal conductivity detector (vario MACRO cube, Elementar, Germany [40]). The oxygen (O) content was determined as the difference of the dry mass subtracted by all elements mentioned above as well as the ash content [33].

Biogas and Methane Potential of Substrates and Determination of Kinetic Parameters The biogas potential (biogas yield, Y_{BG}) and methane potential (methane yield, Y_{CH4}) of the substrates were determined in batch mode according to the VDI 4630 guidelines [41], e.g., as described in [33].

Kinetic parameters were determined by fitting the results to the Modified Gompertz Model (Eq. (3)) [33, 42].

$$P(t) = P_0 \exp \left[-\exp \left(\frac{R_m e}{P_0} (t - \lambda) + 1 \right) \right] \quad (3)$$

$P(t)$ is the cumulative biogas production at time t , P_0 is the maximum biogas yield, R_m is the maximum biogas production rate, t is the time, λ is the lag phase of the digestion, and e is the Euler's number ($e = 2.7182$). The calculations were performed using Python (version 3.12.3). The theoretical biogas ($Y_{BG,theo}$) and methane ($Y_{CH_4,theo}$) potential of the substrates were calculated according to [43].

The characteristics of the substrates are presented in Table 2.

Modeling of the Continuous Digestion Process

This section briefly summarizes the functioning of the model that was to be validated by anaerobic digestion experiments with continuous (daily) substrate addition. It also contains the variables given as input to the model. The original model code, which is written as Python code,

was adapted in a way that it could process multiple substrate changes instead of one, but the basic mathematical processing of the data was not changed. For a detailed explanation of the setup and basic mechanisms of the model, please refer to the original publication [33]. For the present study, calculations were performed using Python (version 3.12.3), the adapted model code is available as specified in the data availability statement.

In general, the model predicts the biogas production using the degradation kinetics of all components of the substrate mix. Hence, the kinetic parameters of the substrates must be determined through batch tests ("Characterization of Substrates" section). Furthermore, it checks some general criteria (e.g., appropriate organic loading rate, C/N ratio) for successfully operating a biogas fermenter. Basic model inputs are shown in Table 3. Specifically, those are operating parameters such as the fermenter volume (VF in Table 3), the hydraulic retention time (HRT1...HRT4 in Table 3), the total time of modeling (tm), the time of substrates changes (tc1...tc3), and the organic loading rate (BR in Table 3). Substrate characteristics from an imported .csv file are stored under coded short names (Substrates1...

Table 2 General characteristics, elemental composition, biogas and methane potential, kinetic parameters, and the respective root mean square error (RMSE) and coefficient of determination (R^2) of the fitted model of all investigated substrates

Substrate	Sugarcane reed I	Lemon leaves	Sugarcane reed II	Grape leaves	Goat dung
General characteristics					
DM (%)	94.8 ± 0.1	93.6 ± 0.02	95.8 ± 0.1	94.7 ± 0.02	93.9 ± 0.4
VS (% _{DM})	92.3 ± 0.01	79.1 ± 0.1	98.6 ± 0.1	78.9 ± 0.2	70.1 ± 1.8
Elemental composition					
C (g kg _{DM} ⁻¹)	440	410	460	400	340
N (g kg _{DM} ⁻¹)	7.3	9.1	2.5	14	15
H (g kg _{DM} ⁻¹)	61	54	63	54	39
S (g kg _{DM} ⁻¹)	< LoQ	< LoQ	< LoQ	< LoQ	< LoQ
O (g kg _{DM} ⁻¹)	414	317	461	321	307
C/N ratio (-)	60.3	45.1	184.0	28.6	22.7
Biogas and methane potential and kinetic parameters					
Y_{BG} (mL _N g _{VS} ⁻¹)	536 ± 25	395 ± 17	505 ± 27	399 ± 15	262 ± 16
CH ₄ content (%)	58.7 ± 0.4	59.9 ± 0.1	63.2 ± 0.5	59.7 ± 0.6	70.0 ± 1.7
Y_{CH_4} (mL _N CH ₄ g _{VS} ⁻¹)	315 ± 25	237 ± 17	319 ± 27	238 ± 43	183 ± 17
$Y_{BG,theo}$ (mL _N g _{VS} ⁻¹)	857	780	895	780	660
$Y_{CH_4,theo}$ (mL _N CH ₄ g _{VS} ⁻¹)	469	453	481	438	337
$Y_{BG}/Y_{BG,theo}$ (%)	63	49	56	51	40
$Y_{CH_4}/Y_{CH_4,theo}$ (%)	67	52	66	54	54
P (mL _N g _{VS} ⁻¹)	504.0	360.2	488.2	382.6	221.3
R_m (mL _N g _{VS} ⁻¹ d ⁻¹)	34.3	34.7	29.8	62.4	10.9
λ (d)	- 2.44	- 2.14	- 1.71	- 0.68	- 1.38
RMSE (mL _N g _{VS} ⁻¹)	21.7	23.1	15.7	21.8	5.8
R^2 (-)	0.97	0.90	0.98	0.92	0.99

<LoQ below limit of quantification

Table 3 Input variables of the model, actual values used in the present study, and a brief explanation for each variable

Variable	Value	Explanation
VF	0.0055	Volume of fermenter (m ³)
HRT1... HRT4	25, 25, 25, 25	Hydraulic retention time of substrate mix 1...4 (d)
tm	292	Time span of the modeling (d)
tc1...tc3	167, 192, 242	Day of substrate change (d)
BR	3	Organic loading rate (g _{VS} L ⁻¹ d ⁻¹)
Substrates1...Substrates4	e.g.: ['SR','LP','GD']	Coded names of substrates mix 1...4 The characteristics are imported via a .csv file that contains data given in Table 1
Shares1... Shares4	e.g.: [0. 5, 0. 5, 0.0]	Shares of substrates in mix 1...4

Substrates4 in Table 3), and the substrate shares within the feedstock mixture must be defined for each substrate mix (Shares1...Shares4 in Table 3).

The information on the substrates' characteristics imported are the water content, volatile solids, C and N content, the kinetic parameters of the anaerobic degradation determined in batch tests, the methane content of the biogas (all "Characterization of Substrates" section), and the respective shares of the substrates (Table 1). The exact values for each parameter and substrate are given in Table 2 ("Characterization of Substrates" section). Characteristics, e.g., the water, volatile solids content, or C/N ratio of the substrate mixture, are derived from the individual substrate characteristics given by the input file according to their share. Generalized, this means that a characteristic X_F of the feedstock mixture is calculated as the sum of the characteristics of the individual substrates $X_{S1}...X_{Sn}$ multiplied by the corresponding share of these substrates $S_{S1}...S_{Sn}$ in the total feedstock mix as shown in Eq. (4) [33].

$$X_F = \sum_{i=1}^n X_{Si}S_{Si} \tag{4}$$

For example, the model derives the C/N ratio of the substrate mixture simply by calculating it from the C and N content of the substrates and their respective shares. Once a threshold is exceeded, it passes a warning about an inadequate C/N_{feed} ratio. This threshold was set to 30 in the original model [33] but increased to 35 in the present investigation based on literature recommendations [10, 16, 17].

Ultimately, the continuous biogas production of the feedstock mixture is predicted via a simple approach: firstly, the cumulative biogas production of each substrate $P_S(t)$ is determined based on the kinetic parameters in the input file using the Modified Gompertz Model (see Eq. (3)). It is used to calculate the daily biogas production rate of each substrate $R_S(t)$ as shown in Eq. (5).

$$R_S(t) = P_S(t) - P_S(t - 1) \tag{5}$$

The daily biogas production rate of the feedstock mixture $R_F(t)$ is then determined with the same approach as the feedstock characteristics, i.e., summing up the individual substrates' biogas production rates $R_{S1}(t)...R_{Sn}(t)$ multiplied by their respective share $S_{S1}...S_{Sn}$ according to Eq. (6).

$$R_F(t) = \sum_{i=1}^n R_{Si}(t)S_{Si} \tag{6}$$

The modeled biogas production rate of the entire reactor $R_M(t)$ is then calculated as the sum of the biogas production rates of all fed batches present in the reactor, hence the total feedstock fed within the past 25 days (=HRT).

To assess the agreement of the model with the experimental data, the following statistical indicators were calculated for the different phases of the experiment: MAE: mean absolute error, RAE: relative absolute error, RMSE: root mean square error, rRMSE: relative root mean square error, R²: coefficient of determination. For evaluating the success of the validation, a criterion was introduced. Considering the uncertainty range of all involved analyses, in particular of the batch experiments (error tolerance of 10% according to [41]) and measurement uncertainties in the biogas volume of the continuous anaerobic digestion system, this criterion was set to a rRMSE of ≤ 10%.

Continuous Anaerobic Co-digestion

Operation of the Anaerobic Digestion Reactor

The continuous anaerobic co-digestion was performed in a lab-scale reactor (BTP2-basic, UIT, Germany, Fig. 2) with a working volume of 5.5 L (full volume: 6.5 L). The plant was equipped with an automated temperature control (heating mantle and temperature probe) and was operated at 37 ± 1 °C. Automated stirring of the reactor content was performed with a propeller agitator once per hour at a speed of 200 min⁻¹ for 5 min. A schematic of the reactor

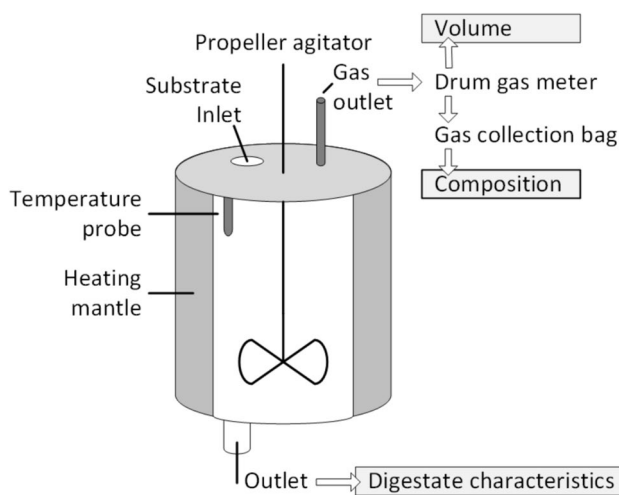


Fig. 2 Schematic of the reactor used for continuous anaerobic digestion experiments

is presented in Fig. 2. For initial inoculation, the reactor was filled with sewage sludge from a wastewater treatment plant located in Seevetal, Germany. The experimental plant was operated at an organic loading rate (OLR) of $3 \text{ g}_{\text{VS}} \text{ L}^{-1} \text{ d}^{-1}$, corresponding to a daily feed of $16.5 \text{ g}_{\text{VS}}$ at a volatile solids content (C_{VS}) of $75 \text{ g}_{\text{VS}} \text{ L}^{-1}$ in the feed mixture. The average hydraulic retention time (HRT) was defined as 25 d corresponding to a flowrate (Q) of 0.22 Ld^{-1} in the investigated system ($V = 5.5 \text{ L}$). This volume was removed daily before feeding an equal amount of fresh substrate mix through an inlet manually. The relationships between these operational parameters are summarized by Eqs. (7) and (8).

$$OLR = (QC_{\text{VS}})/V \quad (7)$$

$$HRT = V/Q \quad (8)$$

The solid and liquid fractions of the removed aliquot were separated via centrifugation (Rotixa 50 RS, Hettich, Germany) to recycle the liquid fraction. The feed added to the reactor once per day consisted of the solid substrates as specified in Table 1 and a mixture of 50% recycled liquid digestate and 50% tap water.

Sample Preparation for Liquid and Solid Phase Analysis

Up to two times per week, the aliquot taken out from the reactor was analyzed for process parameters (“Process Monitoring” section) and digestate characteristics (“Digestate Characteristics” section). For the majority of the analyses performed—and if not stated differently hereafter—the solid and liquid fractions were separated by centrifugation (Rotixa

50 RS, Hettich, Germany). For NH_4^+ and dissolved organic carbon measurements, the samples were filtered through $0.2\text{-}\mu\text{m}$ filters.

Process Monitoring

Biogas Volume and Composition The biogas volume V was measured via a drum gas meter (TG0.5/5, Ritter, Germany). Readings were taken once per day. Additionally, ambient temperature (T) and pressure (p) were noted to convert the biogas volume to volume of dry gas at normal state ($V_{\text{dry},N}$) according to Eq. (9).

$$V_{\text{dry},N} = V \frac{(p - p_w) T_N}{p_N T} \quad (9)$$

T_N is the normal temperature ($T_N = 273 \text{ K}$), p_N is the normal pressure ($p_N = 1013 \text{ hPa}$), and p_w is the water vapor pressure depending on the ambient temperature [41]. The water vapor pressure was calculated using the Magnus formula [44].

The corrected volume ($V_{\text{dry},N}$) was also divided by the time between the measuring points (dt) and referred to the amount of organic mass (m_{VS}) fed to the reactor to obtain the biogas rate ($R_{\text{dry},N}$) as specified in Eq. (10).

$$R_{\text{dry},N} = V_{\text{dry},N}/dt/m_{\text{VS}} \quad (10)$$

For the compositional analysis, the biogas was collected in a gas bag for up to two days and measured with a portable gas analyzer (Biogas 5000, Geotech, UK). It was assumed that the biogas (dry gas in normal state) is composed of CO_2 and CH_4 only.

pH and VFA/TA Ratio The pH of the digestate was measured using a pH probe (pH-Meter 765 Calimatic, Knick, Germany, and HI1131 pH probe, Hanna instruments, Germany). The volatile fatty acids to alkalinity ratio (VFA/TA) was determined by titration with 0.05 M sulfuric acid [45]. This was done manually at the beginning of the experiment. Throughout the experiment, an automatic titrator (HI931 potentiometric titrator with HI1131 pH probe, Hanna instruments, Germany) was used. Since the usage of the automated system did not provide reliable results, the procedure was switched back to manual titration.

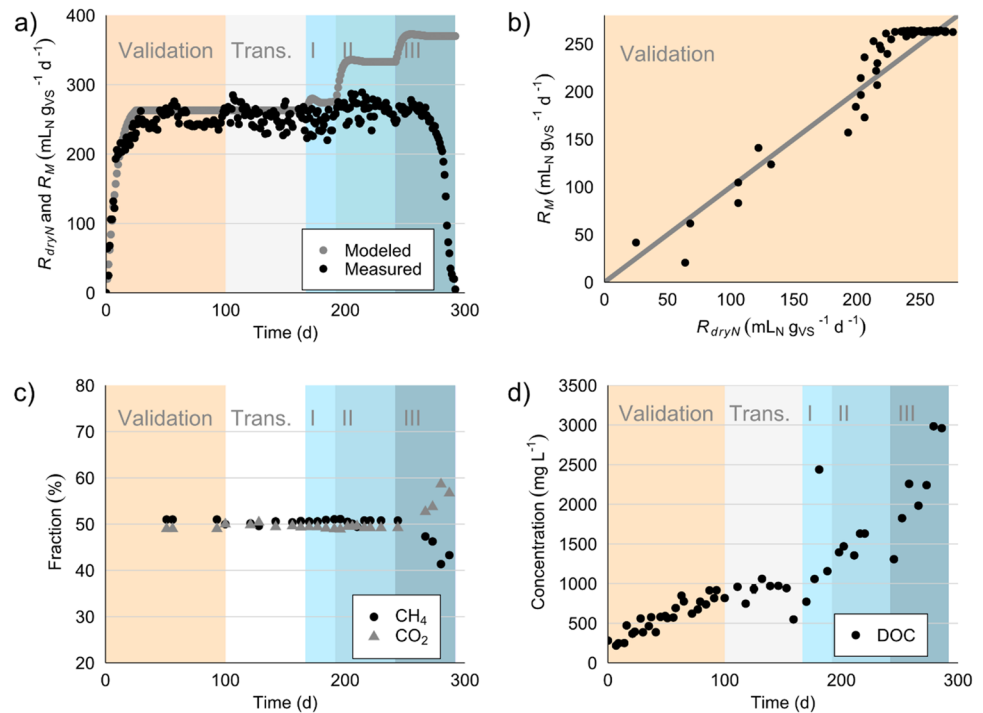
The VFA/TA ratio is calculated according to Eqs. (11), (12), and (13).

$$VFA = ((20/V_s)V_{4.4}1.66 - 0.15)500 \quad (11)$$

$$TA = (20/V_s)V_5250 \quad (12)$$

$$VFA/TA \text{ ratio} = VFA/TA \quad (13)$$

Fig. 3 Monitoring data and digestate characteristics: **a** modeled (R_M) and measured biogas production rate ($R_{dry,N}$). **b** Parity plot of modeled (R_M) and measured biogas production rate ($R_{dry,N}$) in the validation phase. **c** Fraction of CH_4 and CO_2 in biogas. **d** DOC concentration of the liquid digestate. Trans. Transition phase



VFA is the concentration of volatile fatty acids within the digestate and TA is the total alkalinity of the system. V_s is the volume of the sample, $V_{4.4}$ is the volume of sulfuric acid used to titrate from pH 5 to pH 4.4, and V_5 is the volume of sulfuric acid required to titrate to pH 5. Measurements were carried out in triplicates.

Digestate Characteristics

Dry Mass, Volatile Solids, Carbon, and Nitrogen Content The digestate was tested for its dry mass and volatile solids content, as well as the content of C and N in the solid fraction of the digestate. The methods were executed analogously to the analyses performed on the substrates (“Characterization of Substrates” section). The volatile solids removal (VS_r) was calculated from the organic mass given to the reactor (VS_{in}) and the organic mass in the digestate (VS_{out}) as specified in Eq. (14).

$$VS_r = (VS_{in} - VS_{out}) / VS_{in} \cdot 100\% \tag{14}$$

Ammonia Nitrogen The ammonia nitrogen (NH_4^+-N) concentration in the filtered liquid samples was measured photometrically using a test kit (LCK503 and LCK505, Hach Lange, Germany, Photometer: DR 3900, Hach Lange, Germany [46, 47]).

Dissolved Organic Carbon and Total Nitrogen For dissolved organic carbon (DOC) and total nitrogen (TN) measurements, the filtered liquid samples were acidified to a

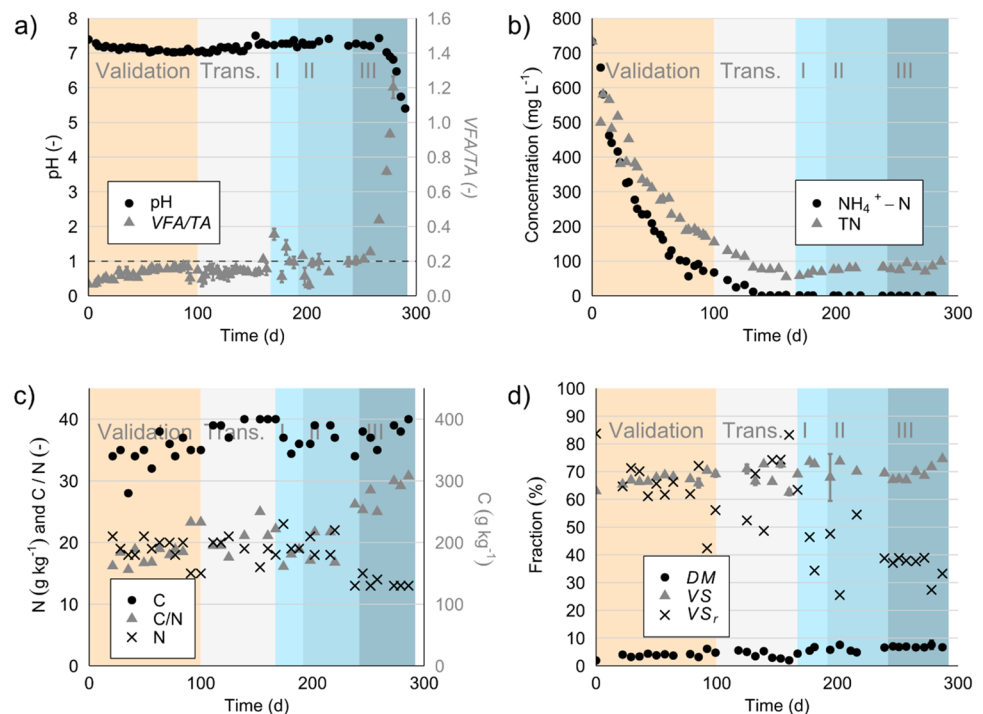
pH-value of < 2 using concentrated phosphoric acid. Measurements were taken in 1:5 diluted samples using a TOC analyzer (multi N/C 3000, Analytik Jena, Germany). The determination was carried out according to DIN EN 1484 [48]. Measurements were carried out in triplicates.

Results and Discussion

Model Validation

Results At the beginning of the continuous anaerobic digestion experiments, the biogas production rate ($R_{dry,N}$) was low and increased steadily during the first 25 d (Fig. 3a). Between days 25 and 99 the biogas production rate reached a level of $250 \pm 10 \text{ mL}_N \text{ g}_{VS}^{-1} \text{ d}^{-1}$ with a methane content of 51% (Fig. 3c). Similar to the biogas production rate, the two process monitoring parameters pH-value and VFA/TA ratio were subjected to change in the very beginning of the startup of the process (Fig. 4a). There was a slight decline in the pH-value starting from 7.4 equilibrating around 7.1 ± 0.1 . The VFA/TA ratio increased throughout the startup phase starting at 0.07 ± 0.02 (day 1) and reaching a level of 0.15 ± 0.01 (day 100). This change in VFA/TA was accompanied by an increase in DOC from $218.5 \pm 2.9 \text{ mg L}^{-1}$ (day 1) to $818 \pm 18.5 \text{ mg L}^{-1}$ (Fig. 3d) and an increase in DM from $1.9 \pm 0.0\%$ (day 0) to $4.8 \pm 0.7\%$ (day 99) and VS content from $63.0 \pm 0.2\%_{DM}$ (day

Fig. 4 Monitoring data and digestate characteristics: **a** pH and *VFA/TA* ratio of the digestate, dashed line represents a *VFA/TA* of 0.2. **b** $\text{NH}_4^+\text{-N}$ and TN concentration of the liquid digestate. **c** N and C content and $\text{C/N}_{\text{digestate}}$ ratio of the solid digestate. **d** *DM* and *VS* of the digestate (not centrifuged) and *VS_r*. Trans. Transition phase



0) to $69.1 \pm 1.1\%_{\text{DM}}$ (day 99) (Fig. 4d). During the validation phase, the volatile solids removal rate *VS_r*, was always higher than 60% (Fig. 4d), indicating effective conversion. Since these parameters remained fairly stable throughout the fourth *HRT*, it can be assumed that a steady state had been established in the reactor.

To validate the predictive model [33], the measured biogas rate ($R_{\text{dry},N}$) was compared to the model predictions (R_M , Fig. 3a). Statistical indicators are presented in Table 4, and a parity plot for the validation phase is shown in Fig. 3b. For validation purposes, the startup and, in particular, the steady-state reached thereafter (i.e., the entire period from day 0 to 99) are considered. Over this entire period, the model predictions showed a close correlation to the measured values with an R^2 value of 0.93 (Table 4). Also, the deviation between the model and experimental data was relatively small with a *RMSE* of $19 \text{ mL}_N \text{ g}_{\text{VS}}^{-1} \text{ d}^{-1}$ and a *rRMSE* of 8%. Throughout the period from day 25 to 99, including the steady state phase, the mean measured biogas rate was $250 \pm 10 \text{ mL}_N \text{ g}_{\text{VS}}^{-1} \text{ d}^{-1}$. This accounts for a *RMSE* of $17 \text{ mL}_N \text{ g}_{\text{VS}}^{-1} \text{ d}^{-1}$ and a *rRMSE* of 7% compared to the model predictions of $263 \text{ mL}_N \text{ g}_{\text{VS}}^{-1} \text{ d}^{-1}$. According to Fig. 3a, the biogas production within the reactor was slightly below the model predictions most of the days; this is especially true for higher biogas rates as shown in Fig. 3b.

Discussion Overall, the changes in the monitoring parameters can be explained by the stepwise increased organic loading of the reactor at the beginning of the experiment. Since the reactor was started with pure inoculum and the

organic loading rate of $3 \text{ g}_{\text{VS}} \text{ L}^{-1} \text{ d}^{-1}$ is only continuously adjusted through the daily feeding, the parameters develop accordingly. This can be seen most clearly in the low but increasing *VFA/TA* ratio; values below 0.2 indicate a very low organic load. As most of the parameters—especially the process monitoring parameters biogas production, pH and *VFA/TA* ratio—stabilized within the startup phase and beyond, it can be concluded that the reactor was in a steady state after three hydraulic retention times.

Taking the error of the batch tests—which are the basis of the model predictions—and an error of the continuous anaerobic digestion—e.g., fluctuations and underestimation of the reactive volume inside the reactor, natural variations in the quality of the feedstock and loss of biogas—with a *rRMSE* of 8%, the measured and modeled data are in good agreement with one another. It must be stressed at this point that the validation conducted was done under optimal conditions in terms of, e.g., C/N_{feed} ratio and organic loading rate. Hence, there was neither a surplus of organic feed material nor an overexpansion of the appropriate range of the C/N ratio. The authors of the model originally suspected the model to give reliable results under favorable conditions. Here, the assumption can be confirmed that under the given conditions, the model is able to predict the biogas production with a *rRMSE* below 10%. The model is therefore classified as successfully validated, fulfilling the validation criterion introduced in the “Modeling of the Continuous Digestion Process” section.

Table 4 Mean, minimum (min), and maximum (max) experimental biogas production rate $R_{dry,N}$, predicted biogas production rate R_M (predicted steady production rate), and statistical indicators assessing the agreement between experimental and modeled data: MAE mean

absolute error, RAE relative absolute error, $RMSE$ root mean square error, $rRMSE$ relative root mean square error, R^2 coefficient of determination

Phase	Validation			Transition	I	II	III
	0–24	25–99	0–99				
Duration (day)				100–166	167–191	192–241	242–291
C/N (-)	33	33	33	33	33	43	52
$R_{dry,N}$ mean ($\text{mL}_N \text{g}_{VS}^{-1} \text{d}^{-1}$)	n.a	250 ± 10	n.a	254 ± 14	246 ± 13	266 ± 12	n.a
$R_{dry,N}$ min ($\text{mL}_N \text{g}_{VS}^{-1} \text{d}^{-1}$)	0	235	0	223	220	234	5
$R_{dry,N}$ max ($\text{mL}_N \text{g}_{VS}^{-1} \text{d}^{-1}$)	244	276	276	285	265	289	278
CH ₄ content	-	50.6 ± 0.5	50.6 ± 0.5	50.3 ± 0.4	50.8 ± 0.2	50.5 ± 0.5	41.4...50.8
R_M ($\text{mL}_N \text{g}_{VS}^{-1} \text{d}^{-1}$)	n.a	263	263	263	274	333	370
MAE ($\text{mL}_N \text{g}_{VS}^{-1} \text{d}^{-1}$)	20	14	16	13	39	64	160
RAE (-)	0.34	1.66	0.52	1.15	2.55	6.88	2.43
$RMSE$ ($\text{mL}_N \text{g}_{VS}^{-1} \text{d}^{-1}$)	24	17	19	16	32	66	180
$rRMSE$ (-)	0.14	0.07	0.08	0.06	0.13	0.25	0.86
R^2 (-)	0.93	n.a	0.93	n.a	n.a	n.a	n.a

n.a. not applicable

Effect of Varied C/N_{feed} Ratio

To evaluate the effect of the varied C/N_{feed} ratio, three operational phases with different C/N_{feed} ratios in the substrate are compared below. The assessment involved the biogas production rate ($R_{dry,N}$, “Biogas Production Rate” section), process monitoring parameters (pH, VFA/TA, “Process Monitoring” section), as well as a closer look at the evolution of nitrogen species in the liquid and solid digestate (“Ammonium and Total Nitrogen in Liquid Digestate and Nitrogen Content of Solid Digestate” section).

Biogas Production Rate

Results During phase I (C/N_{feed} = 33), the daily biogas production rate $R_{dry,N}$ remained constant when compared to the previous operation ranging between 220 and 265 $\text{mL}_N \text{g}_{VS}^{-1} \text{d}^{-1}$ (Table 4, Fig. 3a). The slight increase of biogas production, which was predicted by the model due to the substrate change, could not be observed. Nevertheless, with a mean of $246 \pm 13 \text{ mL}_N \text{g}_{VS}^{-1} \text{d}^{-1}$, the measured biogas production remained close to the predicted production rate of $274 \text{ mL}_N \text{g}_{VS}^{-1} \text{d}^{-1}$ (R_M pred., Table 4). Thereafter, the substrate mix was adapted to a C/N_{feed} ratio of 43, which also meant an increase in the shares of sugarcane reed and grape leaves. Because these two substrates comprise a higher biogas potential in batch tests (Y_{BG} in Table 2) than the goat dung, the model predicted a rise in biogas production to around $333 \text{ mL}_N \text{g}_{VS}^{-1} \text{d}^{-1}$. At this point, the model passed a warning, stating that the C/N_{feed} ratio might be inadequate. Even though there was an observable increase

in biogas production, which was $266 \pm 12 \text{ mL}_N \text{g}_{VS}^{-1} \text{d}^{-1}$ on average (range: 234 to 289 $\text{mL}_N \text{g}_{VS}^{-1} \text{d}^{-1}$) compared to $246 \pm 13 \text{ mL}_N \text{g}_{VS}^{-1} \text{d}^{-1}$ in phase I, the measured biogas production remained clearly below the predictions of the model with a $rRMSE$ of 25% (Table 4, Fig. 3a). After completely fading out the goat dung from the substrate mixture (phase III, C/N_{feed} ratio = 52), the model predicted a rise in biogas production to $370 \text{ mL}_N \text{g}_{VS}^{-1} \text{d}^{-1}$. Again, a warning about the inadequate C/N_{feed} ratio was given by the model. While the substrate change did not affect the biogas production in the first 25 d of phase III (biogas production of $264 \pm 7 \text{ mL}_N \text{g}_{VS}^{-1} \text{d}^{-1}$ compared to $266 \pm 12 \text{ mL}_N \text{g}_{VS}^{-1} \text{d}^{-1}$ in phase II) it declined rapidly thereafter (Fig. 3a). At the end of phase III, the production reached a minimum of $5 \text{ mL}_N \text{g}_{VS}^{-1} \text{d}^{-1}$, and there was a severe miss match between the experimental data and the model with a $rRMSE$ of 86% (Table 4). This process failure was accompanied by a decreasing share of methane content in the biogas (Fig. 3c). While it remained just above 50% during phases I and II, the methane content of the biogas was 43% toward the end of phase III (day 287). Moreover, the VS , indicating the conversion efficiency—which was in the range of 60% under stable conditions and a C/N ratio of 33—was notably diminished with values consistently below 40% in phase III (Fig. 4d).

Discussion Due to the individual combination of substrates and the diversity of biogas substrates in general, a direct comparison with literature is hardly possible. However, a comparison with other publications shows that the maximum biogas yield achieved here ($266 \pm 12 \text{ mL}_N \text{g}_{VS}^{-1} \text{d}^{-1}$ in phase II) is rather low. For example, for the co-digestion

of swine manure and rice straw (mixing ratio 50:50, OLR $3 \text{ g}_{\text{VS}} \text{ L}^{-1} \text{ d}^{-1}$), a biogas production of $380 \text{ mL}_{\text{N}} \text{ g}_{\text{VS}}^{-1}$ ($209.0 \pm 39.1 \text{ mL}_{\text{N}} \text{ CH}_4 \text{ g}_{\text{VS}}^{-1}$, CH_4 -content $55.0 \pm 2.0\%$) is reported [49]. The co-digestion of chicken litter, food waste, and wheat straw (mixing ratio: 35:32.5:32.5) showed a biogas production of $321.6 \pm 13.4 \text{ mL}_{\text{N}} \text{ g}_{\text{VS}}^{-1}$ [50]. For the co-digestion of dairy manure and rice straw (mixing ratio 10:90, OLR $1 \text{ g}_{\text{VS}} \text{ L}^{-1} \text{ d}^{-1}$), a biogas production of $436 \text{ mL}_{\text{N}} \text{ g}_{\text{VS}}^{-1}$ ($222 \pm 5.2 \text{ mL}_{\text{N}} \text{ CH}_4 \text{ g}_{\text{VS}}^{-1}$, CH_4 -content 50.9%) is reported [19]. The differences compared to this study can be explained by the fact that the individual substrates, in this case the goat manure and the leaf biomass, had a comparatively low biogas potential themselves. In the batch tests, the biogas production of some of the individual substrates used in the present study only reached 49% (lemon leaves), 51% (grape leaves), and 40% (goat manure) of the theoretical biogas potential (Table 2). Often, this effect is related to a high lignin content in the biomass, hindering anaerobic conversion and could be reduced by implementing pre-treatment of the lignocellulosic materials [24–26]. Additionally, the residence time in the continuous reactor is shorter than in the batch tests, resulting in underutilization of its full potential.

A detailed consideration of phases II and III and the process breakdown is provided in the discussion of process monitoring parameters (“Process Monitoring” section) and nitrogen parameters (“Ammonium and Total Nitrogen in Liquid Digestate and Nitrogen Content of Solid Digestate” section) in the following. Nevertheless, the mismatch of the model and the measurement data in phases II and III is already obvious. Although the model issued a warning about the inadequate C/N_{feed} ratio, it was not able to predict the breakdown of the biogas process. This shows a significant limitation of the simplified model and confirms the authors’ doubts about the applicability of the model under unfavorable conditions [33]. The conducted model validation can therefore only be regarded as valid for favorable framework conditions, showing improper prediction at C/N ratios exceeding the defined limit of 35. Seen from another angle, the model (or more precisely, the deviation from the model’s prediction) can indicate a process inhibition at an early stage, which could enable rapid intervention in practice. To make use of this feature, a $rRMSE$ of $> 10\%$ between predicted and actual biogas production could function as a threshold for intervention.

Process Monitoring

Results Just as the biogas production, the process monitoring parameters pH-value and VFA/TA ratio underwent changes as phase III ($C/N_{\text{feed}} = 52$) proceeded. It should be noted that the quality of the VFA/TA data between days 160

and 202 (including phase I and the beginning of phase II; Fig. 4a) is not sufficient due to an instrument malfunction, so the data recorded during that phase might not represent the actual conditions in the reactor accurately. Not considering this period, overall, the VFA/TA ratio mainly remained below 0.2 throughout the operation of the plant. On day 252, a VFA/TA ratio of 0.2 (marked as a dashed line in Fig. 4a) was exceeded for the first time.¹ It rapidly surpassed 0.3 (day 266, day 24 of phase III), and as the biogas production declined, it increased further to 0.9 (day 276) and beyond. Looking at the TA and VFA individually, a decline in TA ranging from 90.7 ± 0.9 to $104.6 \pm 1.6 \text{ mg CaCO}_3 \text{ L}^{-1}$ in phases I and II and dropping from above 100 to $28.3 \pm 0.6 \text{ mg CaCO}_3 \text{ L}^{-1}$ at the end of phase III was observed. At the same time, the concentration of VFA rose from mostly below 20 mg L^{-1} in phases I and II to $174.7 \pm 0.0 \text{ mg L}^{-1}$ at the end of the experiment. A drop in pH was only visible after day 273, where the pH-value decreased from around 7.3 ± 0.1 in phase I and phase II to 7.0 (day 273) and further to 5.4 (day 290) at the end of phase III (Fig. 4a).

Discussion Because the fluctuating VFA/TA data was mainly recorded in phase I, in which the substrate mixture is only changed in terms of substrates but neither the shares of substrate type nor the C/N_{feed} ratio changed and because no fluctuations in pH was measured, it is reasonable to assume that the VFA/TA ratio did not undergo strong fluctuations as the data indicates. The VFA/TA ratio throughout phase I and II (mostly below 0.2) is typical for digesters at this organic loading rate [8, 49] and it indicates a stable process with a fairly low organic loading. A VFA/TA ratio of 0.3 is usually the upper range of the tolerable VFA/TA scale [51]. The rise in VFA/TA beyond this value as well as the drop in pH indicate an unbalanced production and consumption of organic acids. The VFA concentration itself is relatively low and can usually be tolerated by microbial communities in anaerobic digesters [52, 53]. For instance, Zealand et al. [19] operated a reactor with a mixture of rice straw and dairy manure at a VFA concentration of $420 \pm 28 \text{ mg L}^{-1}$. Hence, it is reasonable to assume that the buffering capacity of the reactor was insufficient to outbalance the increase of VFA , even though the concentration itself cannot be regarded as excessively high. An increasing load of organic acids means excess protons, which react with the buffer systems, i.e., the carbonate and ammonium buffer, present in the reactor. In the case of the carbonate buffer system, the equilibrium is shifted from bicarbonate (HCO_3^-) toward CO_2 ($\text{pK}_a =$

¹ given that the data between day 160 and 202 does not represent the reactor conditions well as explained previously.

6.36, [13]), which then outgases as CO_2 [51]. This effect is detectable as the share of CH_4 in the biogas decreased and the share of CO_2 increased in parallel to the process failure. Consequently, the bicarbonate buffer system was no longer available to buffer the acids in the reactor.

Ammonium and Total Nitrogen in Liquid Digestate and Nitrogen Content of Solid Digestate

Results Looking at the NH_4^+ -N content in the liquid digestate (Fig. 4b), a decline could be observed from the startup phase continuing toward the end of the operation. While the process monitoring parameters stabilized within one or two retention times, the NH_4^+ -N content continued to decrease thereafter. The sewage sludge contained $733 \text{ mg L}^{-1} \text{ NH}_4^+$ -N, which was steadily flushed out from the system even though the liquid fraction of the digestate was recycled and fed back to the reactor. Precisely, in phase I, the digester had a NH_4^+ -N content of $1.2 \pm 0.2 \text{ mg L}^{-1}$. It decreased from 0.9 to 0.3 mg L^{-1} in phase II and remained below 0.5 mg L^{-1} in phase III. Alongside the NH_4^+ -N, the total nitrogen (TN) concentration in the liquid digestate followed a declining trend starting from TN concentrations of 734 mg L^{-1} toward concentrations below 100 mg L^{-1} through the transition phase (Fig. 4b). Unlike the NH_4^+ -concentration, there was no clear declining trend in TN within phase I (range: 58 to 71 mg L^{-1} , mean: $65 \pm 5 \text{ mg L}^{-1}$), phase II (range: 75 to 82 mg L^{-1} , mean: $79 \pm 3 \text{ mg L}^{-1}$), and phase III (range: 71 to 99 mg L^{-1} , mean: $84 \pm 10 \text{ mg L}^{-1}$).

The N content of the solid digestate fluctuated throughout the experiment as shown in Fig. 4c (e.g., within a range of 18 to $23 \text{ g kg}^{-1} \text{ N}$ in phase I). It only started to decline at the end of phase II and throughout phase III toward an N content of 13 g kg^{-1} (day 287). Overall, the digestate was enriched in N and depleted in C compared to the substrate mixture which had a N content of 12 g kg^{-1} in phase I ($C/N_{\text{feed}} = 33$), 10 g kg^{-1} in phase II ($C/N_{\text{feed}} = 43$) and 8 g kg^{-1} in phase III ($C/N_{\text{feed}} = 52$). Consequently, the C/N ratio of the digestate ($C/N_{\text{digestate}}$) remained below the C/N_{feed} ratio. The maximum $C/N_{\text{digestate}}$ ratio was 31 at the end of phase III (Fig. 4c).

Discussion At the beginning of the experiment, the NH_4^+ -N and TN content of the digestate were driven by the fact that a N-rich inoculum was used to start the process. The NH_4^+ -N content at the start of the experiment generally meets the requirements of anaerobic fermentation processes. At no stage of the experiment a risk of ammonia inhibition, which may occur at high NH_4^+ -N values of 1500 to 3000 mg/L , was encountered. To maintain

sufficient N-supply in the system, Scherzinger et al. [33] speculated whether a recycling of the liquid phase of the digestate could counteract the flushing out of the N forms from the reactor. This, however, could not be confirmed by the experimental data. Literature considers an NH_4^+ -N content higher than 50 to 100 mg/L to be favorable for the degradation process [54]. This value was clearly undershot over the course of the experiment, which firstly means an insufficient N supply. As NH_4^+ is the N-form that can be used by microbes directly, such a low NH_4^+ -N concentration must represent a hindrance to microbial activity. Secondly, it also compromises the buffering capacity of the reactor.

While NH_4^+ was the dominating N-form throughout the startup phase, with almost all dissolved total nitrogen being NH_4^+ -N, other (organic) forms of nitrogen were dominant throughout phases I, II, and III when NH_4^+ was almost consistently below 1 mg L^{-1} . The remaining N fraction can be allocated to amino acids. These are formed during the degradation of proteins and are an intermediate product in the complete degradation toward NH_4^+ [54]. At the same time, they are building blocks of the proteins within the microorganisms themselves. The amino acid content and composition depend largely on the substrate, specifically, the manure used for anaerobic degradation [54].

Overall, the observations show a proper operation of the anaerobic digestion process at a C/N_{feed} ratio of 33, a stable but hindered process at a C/N_{feed} ratio of 43, and a failure of the process at a C/N_{feed} ratio of 52. Looking at the results, it should be considered that observations hold true for the given conditions but might differ under deviating conditions. For example, a different approach to test the adequacy of C/N_{feed} ratios could be to run reactors at a given C/N_{feed} ratio, terminate the procedure, and restart the reactor running it at another C/N_{feed} ratio, instead of transitioning from one C/N_{feed} ratio to the other using the same reactor. This approach would avoid one phase impacting the following phases. However, the present approach also minimized this impact by letting the reactor stabilize for at least 3 HRT. Also, the approach allows for evaluating whether the microbial community can adapt to the stepwise N-deficiency. Nevertheless, from the experimental results, it cannot be concluded that the microbial community has adapted to the reduced nitrogen supply.

One way in which an N deficit can impact the anaerobic degradation process is that the microbial community cannot sustain itself. In the case described here, however, the buffer capacity of the reactor, which was weakened by the low NH_4^+ content and the outgassing of carbonate as CO_2 , appears to have played a decisive role, too. The lack of NH_4^+ eliminated an important agent in the

ammonium buffer system of the reactor, causing the pH value to drop to an unfavorable level for methanogenic microorganisms. This, in turn, inhibited the microbial degradation of the organic acids to CH_4 and CO_2 . The accumulation of organic acids in combination with the failure of the two important buffering systems—carbonate and ammonium—resulted in an even more severe pH drop. These findings are well in accordance with other publications often reporting favorable C/N ratios around 20 to 35 [10, 16, 17]. Gil et al. [22] investigated the effect of a varied C/NP ratio on the methane production of synthetic solutions in a batch mode. They showed that the C/NP ratio only impacted the methane potential at very low ratios (excess N and P) in a negative way. At higher C/NP ratios, the methane production was not impacted strongly [22]. However, the highest C/N ratio studied there was 46, which does not cover typical C/N ratios of lignocellulosic residues. This means they could not have observed a hindrance caused by N-deficiency, as it is documented in the present study at a C/N ratio of 52. Beniche et al. [8] performed co-digestion of food waste and agricultural residues (cabbage and cauliflower leaves and stalks) at low organic loading rates. The mixture with the highest biodegradability and methane yield operated at a C/N ratio of 45; a positive impact was also documented at a C/N ratio of 56 [8]. However, unlike in this study, these observations were not generated in continuous experiments. Remarkably, Zealand et al. [19] operated a continuous anaerobic reactor with 100% rice straw which had a C/N ratio of 60 without encountering unstable or diminished biogas production. At the same time, they reported NH_4^+ to be below the detection limit at all times, and VFA concentrations above 500 mg L^{-1} . These observations contrast with the fact that in literature usually enhanced biogas yields are reported when supplementing substrates with manure [16, 49, 55]. Also, they differ from what was found in the investigation presented here. The authors argued that a balanced C/N ratio will be more important at higher organic loading rates [19]. In general, the findings are highly dependent on the process parameters and substrates used. In addition, it should be noted that the C/N ratios given here can also be adjusted by a deviating combination of substrates. Besides the overall C/N ratio, the nitrogen forms present in the individual substrates will impact the anaerobic process, and consequently, the same C/N ratio will not necessarily result in the same biochemical conditions inside the reactor and thus yield different results. Under the conditions given here, no positive effect—in the sense of additional biogas production—of a balanced C/N

ratio could be determined. The fact that a minimum level of N and thus a certain C/N ratio is required to maintain continuous processes could be demonstrated here. Consequently, the regional, seasonal, and quantitative availability of N-rich substrates as compensation for the low N content of lignocellulosic residues might be a limiting factor for the operation of biogas plants run with lignocellulosic residues. At the same time, this means that a stable process can be maintained through a balanced supply of nutrients during co-digestion.

Conclusion

This study successfully validated the cited model through long-term continuous anaerobic digestion experiments, at the same time demonstrating the viability of using lignocellulosic substrates. The model provided accurate predictions within the limits specified by the original publication. However, increasing the C/N ratio resulted in insufficient N-supply and buffering capacity, compromising process stability and biogas production. Under unfavorable conditions, predictions and actual production showed strong deviation. While this may highlight a limitation of the model, in practice—if model predictions are undershot—this could be used as an indicator for intervention and offers potential for further research and development.

Acknowledgements We express our appreciation to Kinjal Ramavat and Nivedita Ankalgi for their dedication during the lab work, which contributed to the advancement of the research.

Author Contribution Jana Schultz: conceptualization, methodology, software, formal analysis, investigation, writing—original draft, writing—review and editing, and visualization. Marvin Scherzinger: conceptualization, methodology, software, and writing—review and editing. Amr Y. Elbanhaway: resources, supervision, and project administration. Martin Kaltschmitt: resources, writing—review and editing, supervision, project administration, and funding acquisition.

Funding Open Access funding enabled and organized by Projekt DEAL. The authors acknowledge the support for the work published in this paper by the “Co-Agrow +” project, which is co-funded by the German Federal Ministry of Education and Research, and Egypt’s Science, Technology and Innovation Funding Authority, through the Germany-Egyptian Research Fund facility (grant number: 01DH21002/ID: 33664).

Data Availability The data generated during and/or analyzed during the current study is available from the corresponding author on reasonable request.

Code Availability The code of the model and databased used during the current study are available in the repository under the following link: <https://github.com/JanaSchultz/BiogasPrediction>.

Declarations

Competing Interests The authors declare no competing interests.

Open Access This article is licensed under a Creative Commons Attribution 4.0 International License, which permits use, sharing, adaptation, distribution and reproduction in any medium or format, as long as you give appropriate credit to the original author(s) and the source, provide a link to the Creative Commons licence, and indicate if changes were made. The images or other third party material in this article are included in the article's Creative Commons licence, unless indicated otherwise in a credit line to the material. If material is not included in the article's Creative Commons licence and your intended use is not permitted by statutory regulation or exceeds the permitted use, you will need to obtain permission directly from the copyright holder. To view a copy of this licence, visit <http://creativecommons.org/licenses/by/4.0/>.

References

- Searchinger TD, James O, Dumas P et al (2022) EU climate plan boosts bioenergy but sacrifices carbon storage and biodiversity. *Nature* 612:27–30
- IEA (2020) Outlook for biogas and biomethane: prospects for organic growth. https://iea.blob.core.windows.net/assets/03aeb10c-c38c-4d10-bccc-de92e9ab815f/Outlook_for_biogas_and_biomethane.pdf. Accessed 22 Oct 2024
- IEA (2023) Renewables 2023: analysis and forecast to 2028. https://iea.blob.core.windows.net/assets/96d66a8b-d502-476b-ba94-54ffd84cf72/Renewables_2023.pdf. Accessed 22 Oct 2024
- Paramonova K, Mazancová J, Roubík H (2023) Dis-adoption of small-scale biogas plants in Vietnam: what is their fate? *Environ Sci Pollut Res Int* 30:2329–2339. <https://doi.org/10.1007/s11356-022-24047-9>
- Xu N, Liu S, Xin F et al (2019) Biomethane production from lignocellulose: biomass recalcitrance and its impacts on anaerobic digestion. *Front Bioeng Biotechnol* 7:191. <https://doi.org/10.3389/fbioe.2019.00191>
- Manyi-Loh CE, Lues R (2023) Anaerobic digestion of lignocellulosic biomass: substrate characteristics (challenge) and innovation. *Fermentation* 9:755. <https://doi.org/10.3390/fermentation9080755>
- Trujillo-Reyes Á, Serrano A, Cubero-Cardoso J et al (2024) Does seasonality of feedstock affect anaerobic digestion? *Biomass Convers Biorefinery* 14:26905–26914. <https://doi.org/10.1007/s13399-022-03336-w>
- Beniche I, Hungria J, El Bari H et al (2021) Effects of C/N ratio on anaerobic co-digestion of cabbage, cauliflower, and restaurant food waste. *Biomass Convers Biorefinery* 11:2133–2145. <https://doi.org/10.1007/s13399-020-00733-x>
- Fricke K, Santen H, Wallmann R et al (2007) Operating problems in anaerobic digestion plants resulting from nitrogen in MSW. *Waste Manag* 27:30–43. <https://doi.org/10.1016/j.wasman.2006.03.003>
- Mao C, Feng Y, Wang X, Ren G (2015) Review on research achievements of biogas from anaerobic digestion. *Renew Sustain Energy Rev* 45:540–555. <https://doi.org/10.1016/j.rser.2015.02.032>
- Benabdallah El Hadj T, Astals S, Galí A et al (2009) Ammonia influence in anaerobic digestion of OFMSW. *Water Sci Technol J Int Assoc Water Pollut Res* 59:1153–1158. <https://doi.org/10.2166/wst.2009.100>
- Piątek M, Lisowski A, Kasprzycka A, Lisowska B (2016) The dynamics of an anaerobic digestion of crop substrates with an unfavourable carbon to nitrogen ratio. *Bioresour Technol* 216:607–612. <https://doi.org/10.1016/j.biortech.2016.05.122>
- Weinrich S, Nelles M (2021) Basics of anaerobic digestion: biochemical conversion and process modelling. *Deutsches Biomasseforschungszentrum gemeinnützige GmbH, Leipzig*
- Croce S, Wei Q, D'Imporzano G et al (2016) Anaerobic digestion of straw and corn stover: the effect of biological process optimization and pre-treatment on total bio-methane yield and energy performance. *Biotechnol Adv* 34:1289–1304. <https://doi.org/10.1016/j.biortechadv.2016.09.004>
- Hassan AN, Nelson BK (2012) Invited review: anaerobic fermentation of dairy food wastewater. *J Dairy Sci* 95:6188–6203. <https://doi.org/10.3168/jds.2012-5732>
- Wang X, Lu X, Li F, Yang G (2014) Effects of temperature and carbon-nitrogen (C/N) ratio on the performance of anaerobic co-digestion of dairy manure, chicken manure and rice straw: focusing on ammonia inhibition. *PLoS ONE* 9:e97265. <https://doi.org/10.1371/journal.pone.0097265>
- Zhang W, Kong T, Xing W et al (2022) Links between carbon/nitrogen ratio, synergy and microbial characteristics of long-term semi-continuous anaerobic co-digestion of food waste, cattle manure and corn straw. *Bioresour Technol* 343:126094. <https://doi.org/10.1016/j.biortech.2021.126094>
- Guarino G, Carotenuto C, Di Cristofaro F et al (2016) Does the C/N ratio really affect the bio-methane yield? A three years investigation of buffalo manure digestion. *Chem Eng Trans* 49:463–468. <https://doi.org/10.3303/CET1649078>
- Zealand AM, Mei R, Papachristodoulou P et al (2018) Microbial community composition and diversity in rice straw digestion bioreactors with and without dairy manure. *Appl Microbiol Biotechnol* 102:8599–8612. <https://doi.org/10.1007/s00253-018-9243-7>
- Habiba L, Hassib B, Moktar H (2009) Improvement of activated sludge stabilisation and filterability during anaerobic digestion by fruit and vegetable waste addition. *Bioresour Technol* 100:1555–1560. <https://doi.org/10.1016/j.biortech.2008.09.019>
- Zahan Z, Georgiou S, Muster TH, Othman MZ (2018) Semi-continuous anaerobic co-digestion of chicken litter with agricultural and food wastes: a case study on the effect of carbon/nitrogen ratio, substrates mixing ratio and organic loading. *Bioresour Technol* 270:245–254. <https://doi.org/10.1016/j.biortech.2018.09.010>
- Gil A, Siles JA, Serrano A et al (2019) Effect of variation in the C/[N+P] ratio on anaerobic digestion. *Environ Prog Sustain Energy* 38:228–236. <https://doi.org/10.1002/ep.12922>
- Wu X, Yao W, Zhu J, Miller C (2010) Biogas and CH₄ productivity by co-digesting swine manure with three crop residues as an external carbon source. *Bioresour Technol* 101:4042–4047. <https://doi.org/10.1016/j.biortech.2010.01.052>
- Chevalier A, Lamarque J, Sambusiti C et al (2025) Pilot-scale assessment of twin-screw extrusion combined with lime pretreatment to improve semi-continuous biomethane production from corn stover, and potential of produced digestate as fertilizer. *J Environ Manage* 377:124635. <https://doi.org/10.1016/j.jenvman.2025.124635>
- Menardo S, Cacciatore V, Balsari P (2015) Batch and continuous biogas production arising from feed varying in rice straw volumes following pre-treatment with extrusion. *Bioresour Technol* 180:154–161. <https://doi.org/10.1016/j.biortech.2014.12.104>
- Akizuki S, Suzuki H, Fujiwara M, Toda T (2023) Impacts of steam explosion pretreatment on semi-continuous anaerobic digestion of lignin-rich submerged macrophyte. *J Clean Prod* 385:135377. <https://doi.org/10.1016/j.jclepro.2022.135377>
- Xing B-S, Chang X-L, Cao S et al (2023) Long-term in-situ starvation and reactivation of co-digestion with food waste and corn straw in a continuous AnDMBR: performance, sludge characteristics, and microorganism community. *Sci Total Environ* 882:163673. <https://doi.org/10.1016/j.scitotenv.2023.163673>
- Sitthikitpanya N, Ponuanri C, Jomnonkhaow U et al (2024) Unlocking the potential of sugarcane leaf waste for sustainable methane production: insights from microbial pre-hydrolysis and reactor optimization. *Heliyon* 10:e25787. <https://doi.org/10.1016/j.heliyon.2024.e25787>

29. Xing B-S, Chang X-L, Zhang Y et al (2024) A compound enzyme as an additive to a continuous anaerobic dynamic membrane bioreactor for enhanced lignocellulose removal from codigestion: performance, membrane characteristics and microorganisms. *Bioresour Technol* 402:130772. <https://doi.org/10.1016/j.biortech.2024.130772>
30. Yang Z, Larsen OC, Muhayodin F et al (2025) Review of anaerobic digestion models for organic solid waste treatment with a focus on the fates of C, N, and P. *Energy Ecol Environ* 10:1–14. <https://doi.org/10.1007/s40974-024-00343-7>
31. Kegl T, Torres Jiménez E, Kegl B et al (2025) Modeling and optimization of anaerobic digestion technology: current status and future outlook. *Prog Energy Combust Sci* 106:101199. <https://doi.org/10.1016/j.peccs.2024.101199>
32. Ling JYX, Chan YJ, Chen JW et al (2024) Machine learning methods for the modelling and optimisation of biogas production from anaerobic digestion: a review. *Environ Sci Pollut Res* 31:19085–19104. <https://doi.org/10.1007/s11356-024-32435-6>
33. Scherzinger M, Kaltschmitt M, Elbanhaway AY (2022) Anaerobic biogas formation from crops' agricultural residues - modeling investigations. *Bioresour Technol* 359:127497. <https://doi.org/10.1016/j.biortech.2022.127497>
34. Andrade Cruz I, Chuenchart W, Long F et al (2022) Application of machine learning in anaerobic digestion: perspectives and challenges. *Bioresour Technol* 345:126433. <https://doi.org/10.1016/j.biortech.2021.126433>
35. Pererva Y, Miller CD, Sims RC (2020) Existing empirical kinetic models in biochemical methane potential (BMP) testing, their selection and numerical solution. *Water* 12:1831. <https://doi.org/10.3390/w12061831>
36. Ashraf Elgzzar N, Scherzinger M, Schultz J, Elbanhaway AY (2023) An approach for lignocellulosic biomass feedstock selection for anaerobic digestion conversion plants in Egypt. In: ICSC (ed) Proceedings of the International Conference on Smart Cities. Cairo, Egypt, pp 365–376
37. Nakhla DA, Hassan MG, Haggag SE (2013) Impact of biomass in Egypt on climate change. *Nat Sci* 05:678–684. <https://doi.org/10.4236/ns.2013.56083>
38. DIN (2015) Solid biofuels – determination of moisture content. DIN EN ISO 18134. Deutsches Institut für Normung e. V.
39. DIN (2012) Sludge, treated biowaste, soil and waste - sludge, sludge, treated biowaste, soil and waste - determination of loss on ignition loss on ignitio. DIN EN 15935. Deutsches Institut für Normung e. V.
40. Diedrich H (2019) NCHS-Elementaranalyse. M02.001. Version 02. Hamburg. Technische Universität Hamburg, Zentrallabor Chemische Analytik.
41. VDI (2016) Characterisation of the substrate, sampling, collection of material data, fermentation tests. VDI 4630. Verein Deutscher Ingenieure e.V. 13.030.30, 27.190
42. Velázquez-Martí B, Meneses-Quelal OW, Gaibor-Chavez J, Niño-Ruiz Z (2019) Review of mathematical models for the anaerobic digestion process. In: Rajesh Banu J (ed) Anaerobic digestion. IntechOpen
43. Boyle WC (1977) Energy recovery from sanitary landfills - a review. *Microb Energy Convers* 119–138. <https://doi.org/10.1016/B978-0-08-021791-8.50019-6>
44. Sonntag D, Heinze D (1982) Sättigungsdampfdruck- und Sättigungsdampfdichtetafeln für Wasser und Eis, 1. Deutscher Verlag für Grundstoffindustrie, Edition
45. Nordmann W (1977) Die Überwachung der Schlammfäulung. \textquotedbl KA-Informationen für das Betriebspersonal. Beil Zur Korresp Abwasser 3:77
46. Hach Lange GmbH (2020) LCK505 Ammonium. <https://de.hach.com/asset-get.download-de.jsa?id=59535880071>. Accessed 14 Mar 2025
47. Hach Lange GmbH (2020) LCK503 Ammonium. <https://de.hach.com/asset-get.download-de.jsa?id=66538543301>. Accessed 14 Mar 2025
48. DIN (2019) Water analysis - guidelines for the determination of total organic carbon (TOC) and dissolved organic carbon (DOC). DIN EN 1484. Deutsches Institut für Normung e. V.
49. Jiménez J, Theuerl S, Bergmann I et al (2016) Prokaryote community dynamics in anaerobic co-digestion of swine manure, rice straw and industrial clay residuals. *Water Sci Technol J Int Assoc Water Pollut Res* 74:824–835. <https://doi.org/10.2166/wst.2016.170>
50. Zahan Z, Othman MZ (2019) Effect of pre-treatment on sequential anaerobic co-digestion of chicken litter with agricultural and food wastes under semi-solid conditions and comparison with wet anaerobic digestion. *Bioresour Technol* 281:286–295. <https://doi.org/10.1016/j.biortech.2019.01.129>
51. Palacios-Ruiz B, Méndez-Acosta HO, Alcaraz-González V et al (2008) Regulation of volatile fatty acids and total alkalinity in anaerobic digesters. *IFAC Proc* 41:13611–13616. <https://doi.org/10.3182/20080706-5-KR-1001.02305>
52. Zhao J, Li Y, Euverink GJW (2022) Effect of bioaugmentation combined with activated charcoal on the mitigation of volatile fatty acids inhibition during anaerobic digestion. *Chem Eng J* 428:131015. <https://doi.org/10.1016/j.cej.2021.131015>
53. Zhang W, Li L, Wang X et al (2020) Role of trace elements in anaerobic digestion of food waste: process stability, recovery from volatile fatty acid inhibition and microbial community dynamics. *Bioresour Technol* 315:123796. <https://doi.org/10.1016/j.biortech.2020.123796>
54. Deng L, Liu Y, Wang W (2020) Biogas technology. Springer Singapore, Singapore
55. Xavier CAN, Moset V, Wahid R, Møller HB (2015) The efficiency of shredded and briquetted wheat straw in anaerobic co-digestion with dairy cattle manure. *Biosyst Eng* 139:16–24. <https://doi.org/10.1016/j.biosystemseng.2015.07.008>

Publisher's Note Springer Nature remains neutral with regard to jurisdictional claims in published maps and institutional affiliations.

Authors and Affiliations

Jana Schultz¹  · Marvin Scherzinger¹  · Amr Y. Elbanhaway²  · Martin Kaltschmitt¹ 

✉ Jana Schultz
jana.schultz@tuhh.de

¹ Institute of Environmental Technology and Energy Economics (IUE), Hamburg University of Technology (TUHH), Eissendorfer Straße 40, Hamburg 21073, Germany

² Energy Technology and Climate Change Laboratory (ETCC), Department of Mechanical Power Engineering, Ain Shams University (ASU), Elsarayt Street 1, Abbasia, Cairo, Egypt